



Thermal studies and influence of the thermal decomposition on dielectric properties of a new coumarin copolymers

Fatih Biryan¹ · Güzin Pihtili² · Kadir Demirelli¹

Received: 20 July 2019 / Accepted: 31 October 2019 / Published online: 16 November 2019
© Akadémiai Kiadó, Budapest, Hungary 2019

Abstract

In this study, firstly 7-hydroxy-4-chloroethyl coumarin compound was synthesized in accordance with the literature (Peterson et al. in *Macromol Chem Phys* 202: 775–784, 2001). Then, this compound was reacted with acryloyl chloride to form the 4-(chloromethyl)-2-oxo-2H chromen-7-yl-acrylate) monomer. A series of copolymers were prepared using this monomer and *n*-butyl acrylate monomer. TGA analysis system was used to examine the thermal properties of homopolymers and copolymers. The activation energies were calculated for thermal decomposition of homopolymer and certain copolymers according to Flynn–Wall–Ozawa method. TGA measurements were taken at different heating rates and given comparatively. The glass transition temperatures of the copolymers were determined by DSC analysis and these results were given comparatively. For investigating the dielectric properties of copolymers, dielectric constant, dielectric loss factor, and ac conductivity values were calculated in the range of 100 Hz–20 kHz frequencies. The results were plotted as a function of frequency. In addition, dielectric behaviors of residues were determined after heating to the first decay temperature of the two-stage decay polymers and compared with the first states.

Keywords Coumarin · Thermal study · Thermal decomposition

Introduction

Thermal degradation of polymers has been an important part of thermal analysis studies in recent times [1–3]. Thermogravimetric analysis (TGA) is a widely used method to study the kinetics of polymer degradation [1]. In thermal decomposition of polymers, depolymerization is one of the main examples of degradation. The distinguishing feature of depolymerization is the absence of residues at elevated temperatures. All degradation products, for example; monomers, dimers, chain moieties, have the same combination with the repeating unit [4]. The Flynn–Wall–Ozawa method is a model-free method. It is plotted against $1/T \ln \beta$ obtained by curves recorded at various heating rates. The Flynn–Wall–Ozawa method is potentially suitable for use in systems with many reactions where activation energy may

vary over time [5]. The isoconversional methods are always applied based on data from multiple heating rates and as a function of transformation [6]. Another of the most popular way of determining the kinetic parameters by thermal analysis is the Kissinger method [7]. The activation energy (E_a) obtained from the slope of the straight lines $\ln(\beta/T_{\max}^2) - 1/T_{\max}$ [8].

Dielectric properties of polymers have been broadly examined. It demonstrates the potential for the development of electronic or optoelectronic application technologies and for electronic applications. Dielectric variability in polymers is because of electronic, molecular, ionic, and interfacial polarization. Polymer materials can be defined by electrical parameters [9, 10].

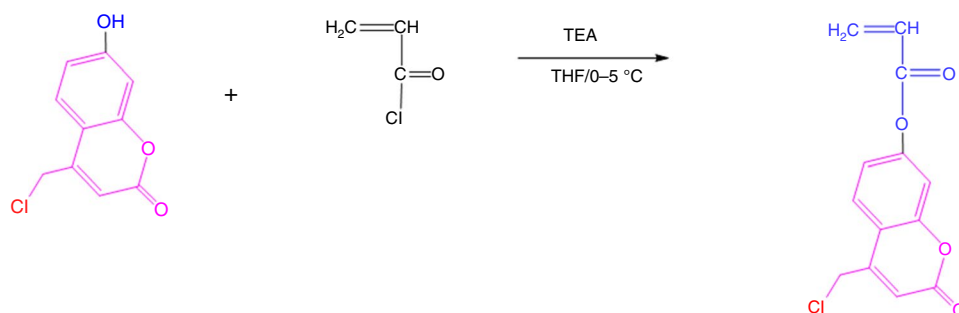
In this work, we synthesized 4-(chloromethyl)-2-oxo-2H chromen-7-yl-acrylate) (CUMAC) as a monomer. And it reacts with *n*-butyl acrylate in five different rates copolymers using free radical polymerization method. And poly (CUMAC-*co*-BA) was synthesized. The thermal degradation behavior of P (CUMAC-*co*-BA) has been determined by using TGA. Our main goal is to determine the dependency of activation energy on Flynn–Wall–Ozawa analysis method. The dielectric measurements of poly

✉ Güzin Pihtili
gpihtili@munzur.edu.tr

¹ Science Faculty Department of Chemistry, Firat University, Elazığ, Turkey

² Pertek Sakine Genç Vocational School, Department of Food Processing, Munzur University, Tunceli, Turkey

Scheme 1 Synthesis procedures of CUMAC monomer



(CUMAC-*co*-BA) were investigated via impedance analyzer at 100 Hz and 30 kHz depending on the alternating current (AC) conductivities. It has been examined that the dielectric constant of residue polymer at 320 °C during thermal degradation of P(CUMAC-*co*-BA).

Materials

Resorcinol, ethyl-4-chloroacetoacetate, *n*-butyl acrylate (BA), acryloyl chloride and sodium hydroxide (NaOH) were supplied from Sigma-Aldrich. They were used as received. Dicumyl peroxide (DCP) was used as initiator, and it was of analytical purity. Tetrahydrofuran, triethylamine (Et₃N), and diethyl ether were used as received without purification. The other materials were used as received commercially and they were of analytical purity.

Instruments

The FTIR spectra were recorded by a Mattson 1000 FTIR in the range 4000–400 cm⁻¹ by preparing films on the NaCl windows. The ¹H NMR and ¹³C NMR spectra were recorded by AVANCE III 400 MHz Bruker NMR spectrometer, using as solvent CDCl₃. The TGA curves were recorded using with a Shimadzu TGA-50. The measurements of TGA applied at a heating rate of 10 °C min⁻¹ from room temperature to 600 °C and DSC-50 at a heating rate of 20 °C min⁻¹ from room temperature to 200 °C. All measurements were taken under dynamic nitrogen atmosphere (under flow of 10 mL min⁻¹). The dielectric measurements were recorded using a QuadTech 7600 LRC impedance analyzer.

The standard method for synthesis of 7-hydroxy-4-chloroethyl coumarin

This compound was synthesized in accordance with the literature [11].

Synthesis of 4-chloromethyl-2-oxo-2H chromen-7-yl-acrylate (CUMAC) monomer

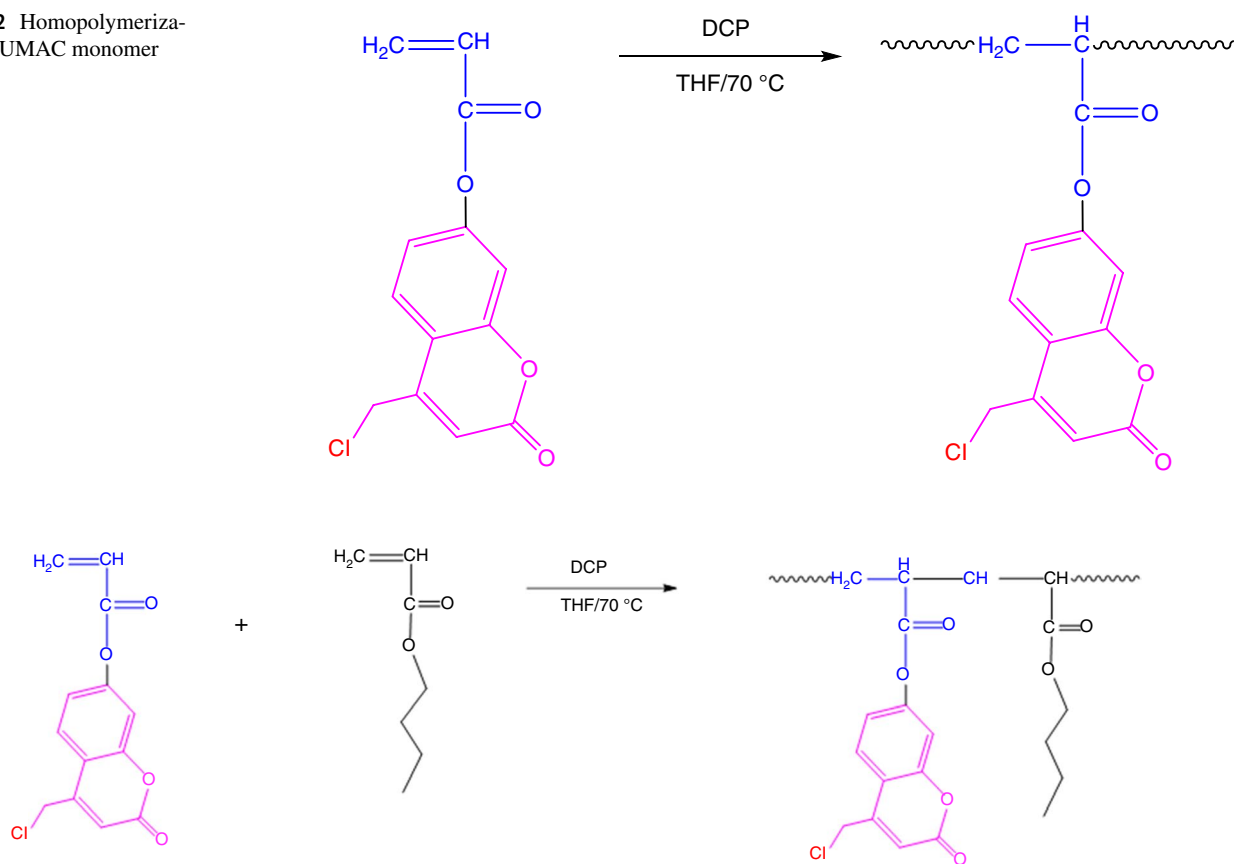
The (CUMAC) monomer was synthesized from the reaction of 7-hydroxy-4-chloroethyl coumarin (3 g, 14.24 mmol) and triethylamine (Et₃N) (1.20 g, 14.96 mmol) in dry tetrahydrofuran (THF) (25 mL). The medium was brought to 0–5 °C with an ice bath. Triethylamine (Et₃N) was used as the adsorbent of the HCl formed during the reaction. Then, the 1.08 g (14.90 mmol) acryloylchloride was slowly added to the reaction medium within 30 min. The mixture of the reaction was stirred at room temperature for 12 h. The formed triethyl ammonium chloride salt was filtrated from the product. The solution of monomer was isolated from the dichloromethane by the evaporator. The monomer was isolated by precipitating within excess water. Finally, the product was dried under vacuum. Synthesis of monomer is illustrated in Scheme 1.

Polymerization of CUMAC monomer

The homopolymerization of CUMAC monomer was carried at 70 °C in the presence of tetrahydrofuran using dicumyl peroxide (DCP) as the initiator. About 0.5 g of the monomer, DCP and 1.5 mL tetrahydrofuran as the solvent were mixed within a polymerization tube. The mixture was passed through argon gas for 15 min and then within an oil bath to 70 °C. The polymerization was terminated after 36 h. The homopolymer was solved in THF and isolated by precipitating within excess ethyl alcohol and purified by reprecipitation. It was dried under vacuum at 40 °C for 24 h. The structure of P(CUMAC) is shown in Scheme 2.

Copolymerization of CUMAC with *n*-butyl acrylate

Poly (CUMAC-*co*-BA) was prepared according to FRP procedure in the presence of THF using DCP as an initiator at 70 °C for 24 h. A certain amount of the monomers, DCP, and THF as a solvent were mixed within a polymerization tube. The prepared mixtures were passed through argon gas for 10 min and then incubated in an oil bath to 70 °C. In these

Scheme 2 Homopolymerization of CUMAC monomer**Scheme 3** Free radical polymerization of CUMAC and *n*-butyl acrylate

conditions, a series of copolymers of different ratios were synthesized. The products were isolated by precipitating within excess ethyl alcohol and purified by reprecipitation. Copolymer systems were dried under vacuum at 40 °C for a day. The structure of copolymer was illustrated in Scheme 3.

Results and discussion

Structure characterization

4-(Chloromethyl)-2-Oxo-7-hydroxy-2H-chromen-2-one was achieved according to the literature [11]. The FTIR spectrum of the compound has an aromatic ring C–H stretching vibration 3068 cm^{-1} , –OH stretching 3248 cm^{-1} , aliphatic C–H stretching vibration at 2950 cm^{-1} . The signal at 10.5 ppm attributed to –OH, 7.69–6.40 ppm was aromatic ring protons, and the peaks at 4.93 ppm assigned to –CH₂–Cl protons. The ¹H NMR spectrum of CUMAC indicates the characteristic signals at 7.95–6.89 ppm

aromatic ring protons (protons on coumarin ring), at 6.16 and 5.65 ppm cis and trans protons on vinyl group, respectively. The ¹H NMR spectrum of monomer is illustrated in Fig. 1a, and ¹³C NMR spectrum of a monomer is shown in Fig. 1b, and they showed the important signals at 165.39 ppm (C=O carbon in the vinyl group), 160.27 ppm (C=O pyron carbon in coumarin units), 167.78 ppm (ester C=O), 155.0–111.2 ppm (carbon on aromatic ring), and 129.2 ppm (CH₂=CH cis and trans carbons). The ¹H NMR spectrum of poly(CUMAC) which is displayed in Fig. 2 demonstrated the most characteristic signals at 7.89–6.9 ppm (aromatic protons in coumarin unit), 4.97 ppm (–CH₂ protons next to the Cl), 1.61–2.66 ppm aliphatic protons in the main chain. FTIR spectra of CUMAC-BA copolymer systems and homopolymer are given in Fig. 3a. The assigned peak in the IR spectrum 3085–3010 cm^{-1} (=C–H stretching on the aromatic ring), 1684 cm^{-1} (–OC=O stretching in coumarin unit), 1608–1564 cm^{-1} (C=C double bond stretching vibration on aromatic), 1136 cm^{-1} (C–O asymmetric stretching), 780 cm^{-1} C–Cl stretching in coumarin unit),

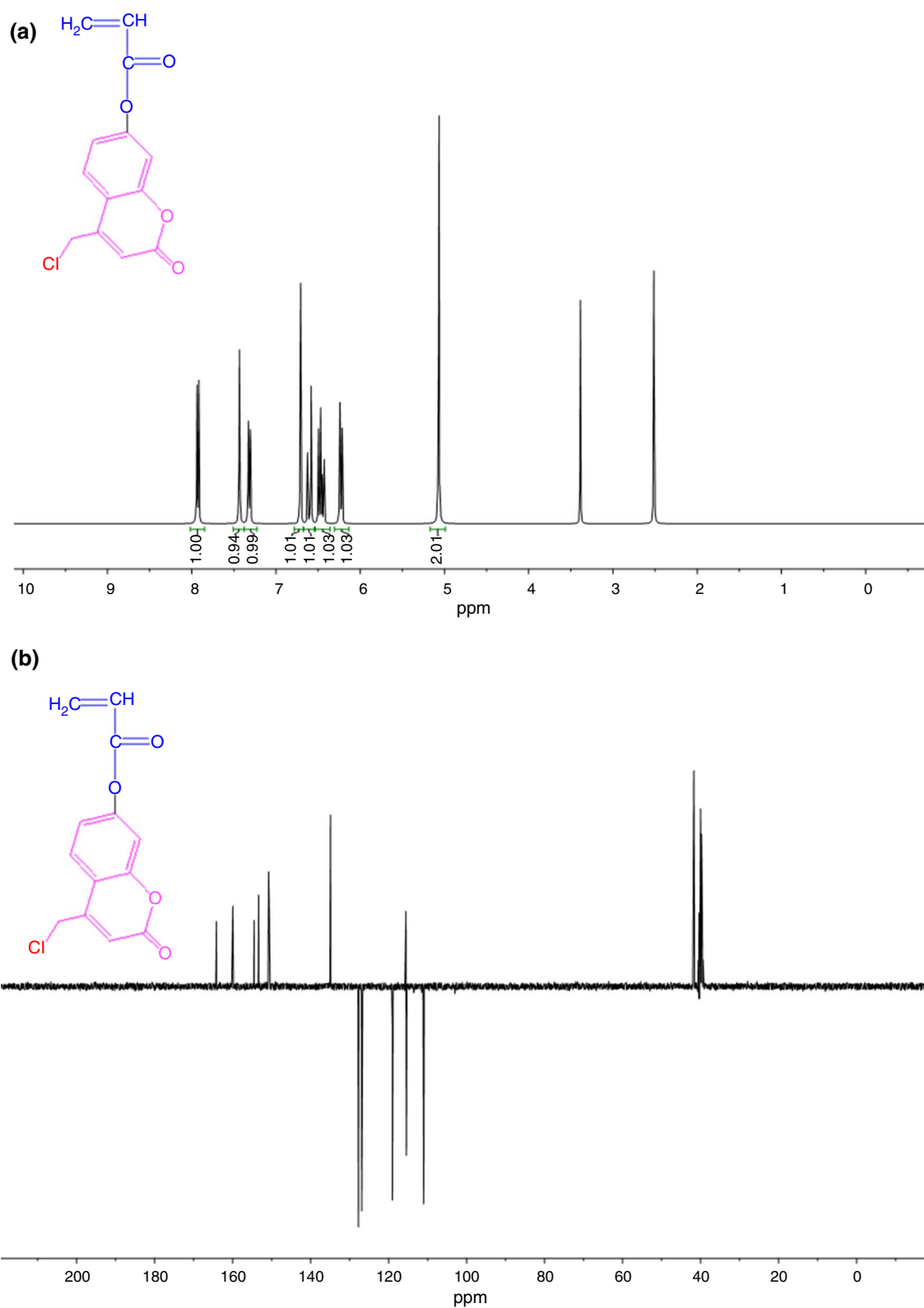
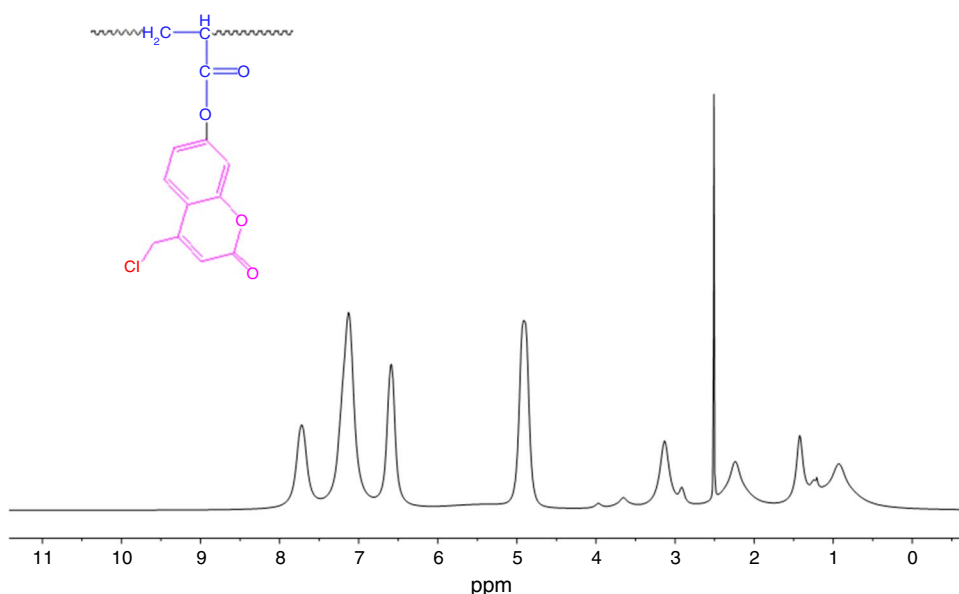


Fig. 1 a ^1H NMR spectrum; b ^{13}C NMR spectrum of CUMAC monomer (d_6 -DMSO)

Fig. 2 ^1H NMR spectrum of Poly(CUMAC)



2995–2951 cm^{-1} (aliphatic C–H stretching in BA unit), 1735 cm^{-1} (OC=O acrylate ester carbonyl), respectively. Figure 3a shows that as the BA units in copolymer system increase, the signal intensity of aliphatic C–H stretching in BA unit is increasing. All the CUMAC-BA copolymer systems showed at 6.59–7.98 ppm (aromatic protons in coumarin unit), 5 ppm ($\text{CH}_2\text{-Cl}$ protons), 3.98 ppm (CH_2 protons in BA unit). As the CUMAC units in copolymer system increase, the signal intensity of $\text{CH}_2\text{-Cl}$ protons in CUMAC unit is increasing. The ^1H NMR spectrum of copolymer system is shown in Fig. 3b, and ^{13}C NMR spectrum recorded only for P(CUMAC-co-BA 0.54) is shown in Fig. 4. Measurement of the ^{13}C NMR spectrum in high concentrations causes the spectrum to be better. The ^{13}C NMR spectrum of the copolymer showed the most characteristic signals at 172.3 ppm (C=O carbon), 66.01 ppm (O– CH_2 carbon in n-BAC unit), 40.7 ppm (Cl– CH_2 carbon in coumarin unit), and 38.7 ppm (quaternary carbon on the main backbone). The copolymer compositions were calculated by the integral height of the CH_2 peak in BA unit at 3.98 ppm and Cl– CH_2 peak in CUMAC at 5 ppm in the H NMR spectrum.

DSC measurements

The glass transition (T_g) temperatures of the homopolymers and copolymers were determined using differential scanning calorimetry (DSC) curves. T_g temperature of amorphous polymers is interested in chain flexibility. This temperature is important and characteristic for polymers because to understand the segmental chain mobility of polymer [12, 13]. The transition does not appear suddenly at a single temperature. It occurs in a temperature range. DSC measurements were

carried out at a heating rate of 20 $^\circ\text{C min}^{-1}$ in under nitrogen atmosphere from room temperature to 200 $^\circ\text{C}$. Since the (T_g) temperature of *n*-butyl acrylate was very low, it was measured by going to low temperatures for the polymers (e) and (d) with liquid nitrogen. DSC curve of (co)polymers was created using a DSC-50. The T_g s of poly (CUMAC) and Poly (CUMAC-co-BA) were received as midpoint of transition region on DSC curve. DSC results of polymers are given in Fig. 5. The T_g s of homopolymers of BA and CUMAC are -48.44 $^\circ\text{C}$ and 120.71 $^\circ\text{C}$, respectively. The T_g temperatures of the copolymers were monitored between the T_g 's of the homopolymers. The T_g values of copolymer system varied from -16.63 $^\circ\text{C}$ to 99.71 $^\circ\text{C}$. There is a formation of the homogeneous phase. This means that the two monomers are compatible with each other. Another important point, as the coumarin content in the copolymer increases, T_g of the copolymer systems to increase against the higher value (Fig. 6). In the CUMAC-BA copolymer systems, it was observed that the BA moieties decreased the chain mobility and free volume so that the T_g temperature will increase.

Thermogravimetric measurements and thermal decomposition kinetics

The thermogravimetric curve of CUMAC-BA copolymers system and P(CUMAC) was obtained from room temperature to 600 $^\circ\text{C}$ at a heating rate of 10 $^\circ\text{C min}^{-1}$ under N_2 flow by TGA. From the TG curves, degradation temperatures were read. Figure 7 shows the non-isothermal TG curves and as a comparison to that of poly (CUMAC) and CUMAC-BA copolymers system prepared by the free radical

Fig. 3 **a** FTIR spectrum; **b** ^1H NMR spectrum of CUMAC-BA copolymer systems

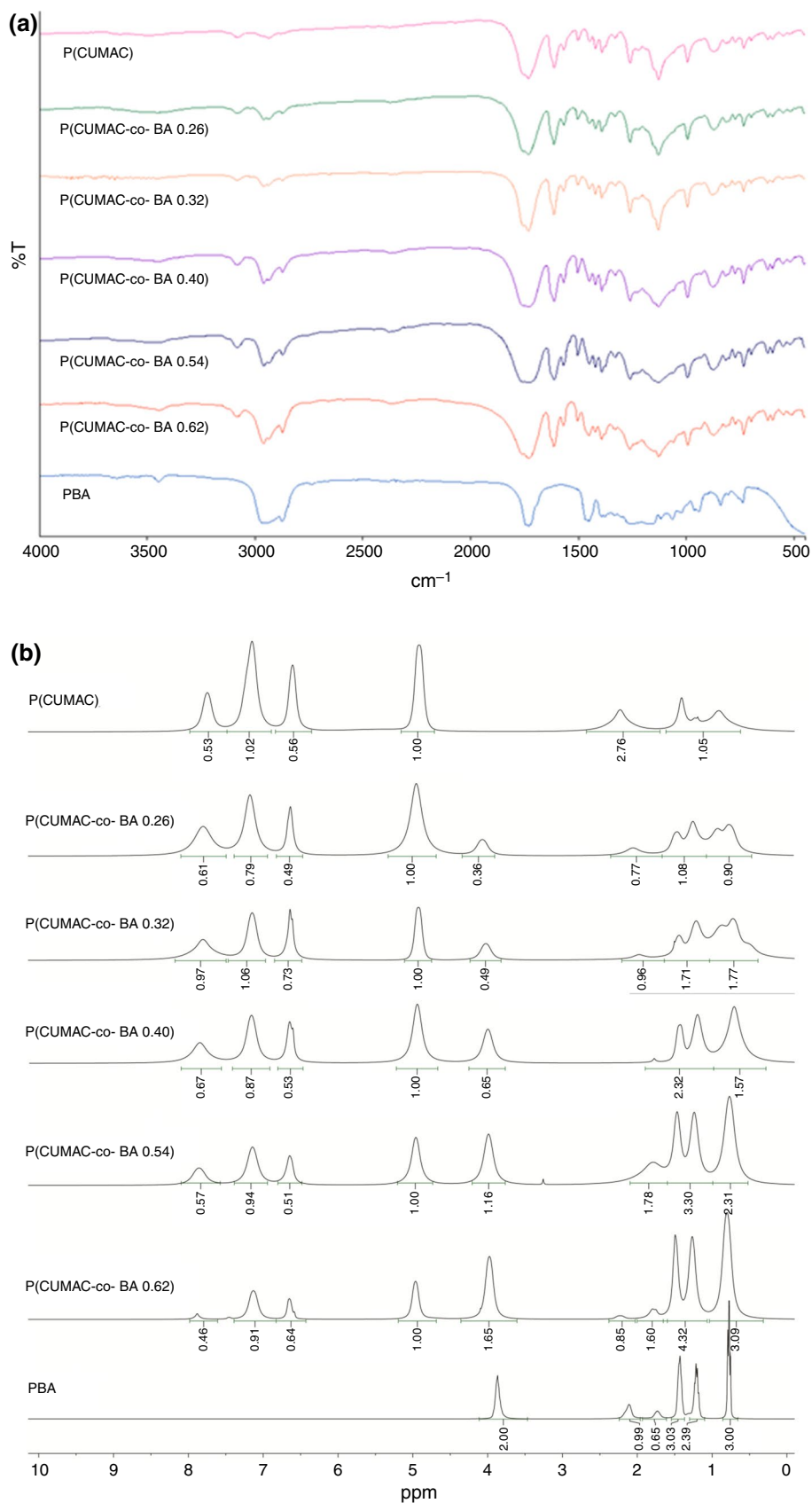


Fig. 4 ^{13}C NMR spectrum of P (CUMAC-co-BA 0.54) (d-chloroform)

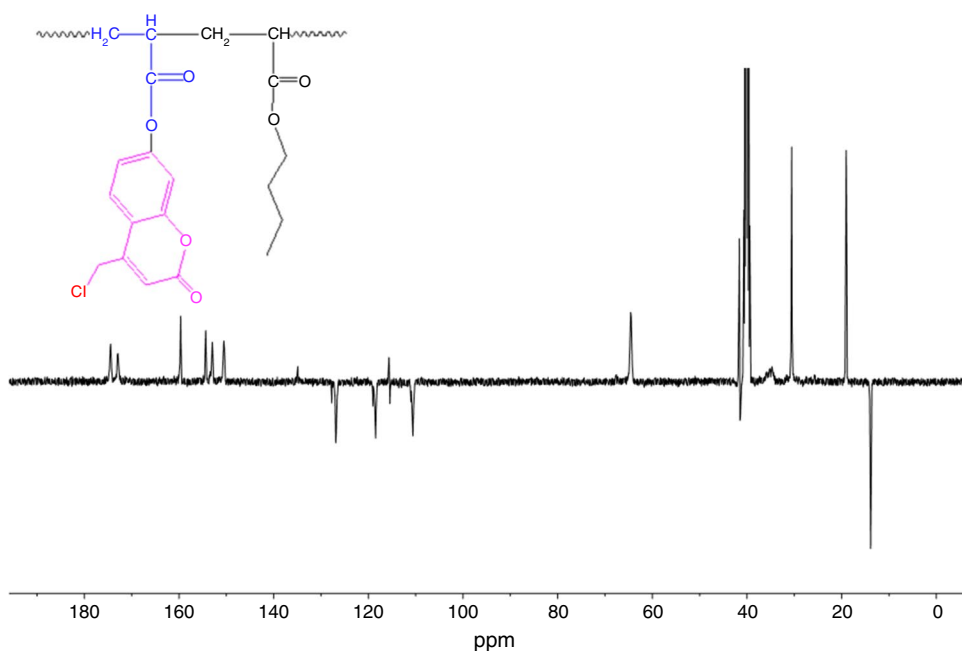


Fig. 5 DSC curve of **a** P(CUMAC); **b** Poly(CUMAC-co-BA 0.26); **c** Poly(CUMAC-co-BA 0.32); **d** Poly(CUMAC-co-BA 0.40); **e** Poly(CUMAC-co-BA 0.54); **f** Poly(CUMAC-co-BA 0.62); **g** P(BA)

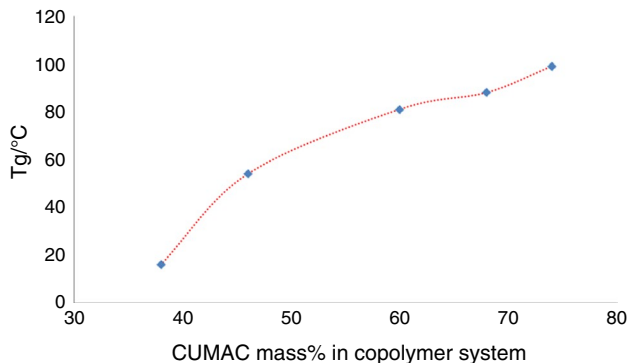
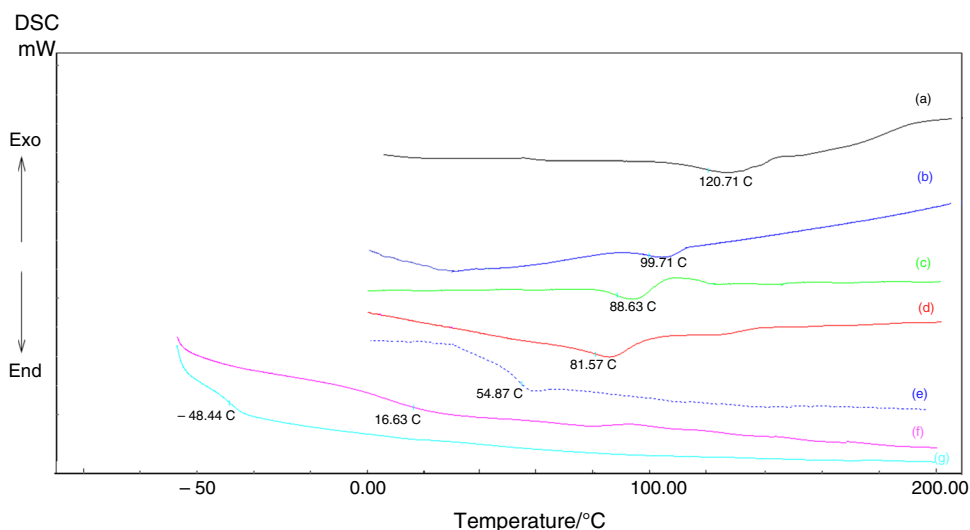


Fig. 6 T_g value against of coumarin content

polymerization method. Decomposition of P(CUMAC) was found to occur in three stages. The initial and final degradation temperatures are: 290–340 °C for the first stage, 375–450 °C for the second stage and 478–520 °C for the third stage. The TGA curves show three-stage decomposition for all copolymer systems too. The first thermal degradation occurred in the range of 250–370 °C. In this stage, the volatile species were completely degraded. At the first stage of TGA, a maximum mass loss of 83.83%, at the second stage a maximum mass loss of 42.73% between 305 and 350°C, and at the third stage, a maximum mass loss of 6.81% between 452 and 475°C were monitored for CUMAC-BA copolymers system. As the coumarin content in the copolymer increased, thermal stability was also increased.

Fig. 7 TGA curves of CUMAC-BA copolymer systems

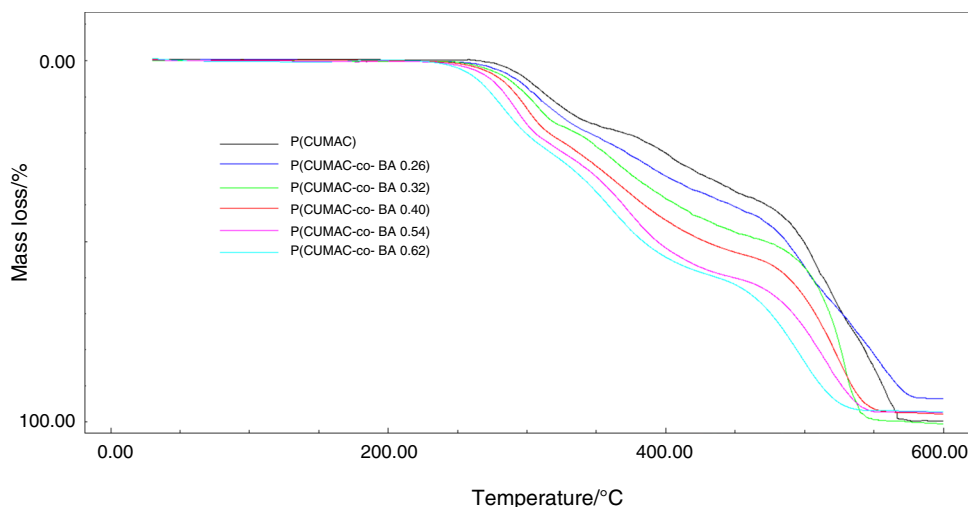


Table 1 TGA data for poly(CUMAC) and copolymers

Polymer	IDT _a /°C	T _{max} /°C	Residue/% at 320/°C	Residue/% at 450/°C
P(CUMAC)	290	560	5	37
Poly(CUMAC-co-BA 0.26)	285	575	10	42
Poly(CUMAC-co-BA 0.32)	280	550	12	48
Poly(CUMAC-co-BA 0.40)	265	545	16	53
Poly(CUMAC-co-BA 0.54)	260	540	18	59
Poly(CUMAC-co-BA 0.62)	250	535	22	63

IDT: Initial decomposition temperature

T_{max}: Temperature at maximum rate of decomposition

The TG results of poly(CUMAC) and the others are summarized in Table 1.

To examine the effect of thermal activation on non-isothermal decomposition kinetics of P(CUMAC-co-BA 0.54) and P(CUMAC-co-BA 0.32) using thermogravimetric analysis according to Flynn–Wall–Ozawa (FWO) method. The forecast of kinetic parameters for thermal decomposition processes was used to understand the degradation process [14, 15]. Activation energy is considered to be one of the most useful parameters [16, 17]. Ozawa–Flynn–Wall is the most common differential isoconversional model [5]. This method performed to compute the kinetic features based on the experimental results without knowing the reaction model [18]. FWO method is an integral method for determining the activation energy without the need to know the reaction order and the degradation mechanism [19, 20]. FWO was derived from the integral method that can establish the activation energy for given

values of conversion [4, 21, 22]. It is the non-isoconversional method, and it is known as a “model-free” method. This method measures dependences $E_a - \alpha$ computed from the data simulated as a function of T from experimental at different heating rates, β , and plotting $\ln(\beta)$ versus $1/T$ [5, 23–25]. The plot of $\ln \beta$ versus $1/T$ gives a straight line with slope $-1.052E_a/R$ [5]. The influence of thermal activation decomposition kinetics was examined according to Flynn–Wall–Ozawa method. All of TGA measurements were carried out non-isothermal methods for the kinetic study and calculated activation energy values (E_a) according to the literature [9, 26]. FWO method is widely used in the literature. The results of FWO analysis ($\ln \beta$ versus $1/T$ curves) obtained from a series of experiments performed at various heating rates (5, 10, 20, 30, and 40 °C min⁻¹) for the conversion values for range from 2 to 50% were estimated for P(CUMAC-co-BA 0.54) and P(CUMAC-co-BA 0.32). The activation energy (E_a) of thermal decomposition is calculated according to Eq. (1).

$$\ln \beta = \log \frac{\Delta E}{\rho(\alpha) \cdot R} - 2.35 - \frac{0.457E}{RT} \quad (1)$$

where β is the heating rate (°C min⁻¹) and R (8.314 J mol⁻¹ K⁻¹) is a constant, α is the extent of conversion, E activation energy (E_a). The values of a have been determined from the TGA data as partial mass losses [4, 5, 9]. The FWO plots of P(CUMAC-co-BA 0.54) using different heating rates (5, 15, 25, 30, and 40 °C min⁻¹) are illustrated in Fig. 8a. The activation energy was calculated at different conversion from 2 to 50%. The results of Flynn–Wall–Ozawa analysis ($\ln \beta$ versus $10^3/T$) are shown in Fig. 8b. The activation energies were found to be 89.38, 96.08, 100.42, 106.21, 104.99, 99.76, 100.25, 104.9, 102.55, 123.27, 117.94, 124.99, 135.61, 185.82, 167.86, 228.10 kJ mol⁻¹ at conversions 0.02, 0.05, 0.08, 0.1, 0.12, 0.15,

Fig. 8 **a** TGA curves in different heating rates of P(CUMAC-co-BA 0.54) **b** the results of Flynn–Wall–Ozawa analysis ($\ln\beta$ vs. $10^3/T$)

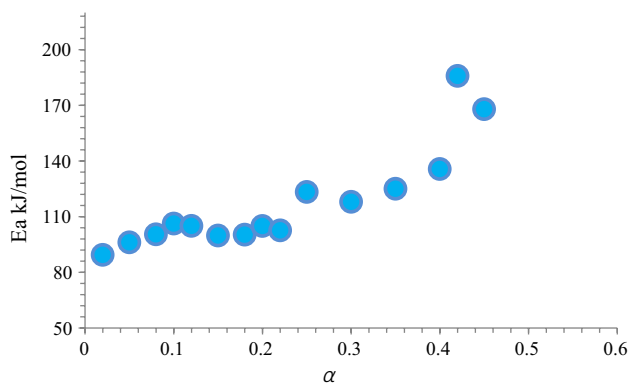
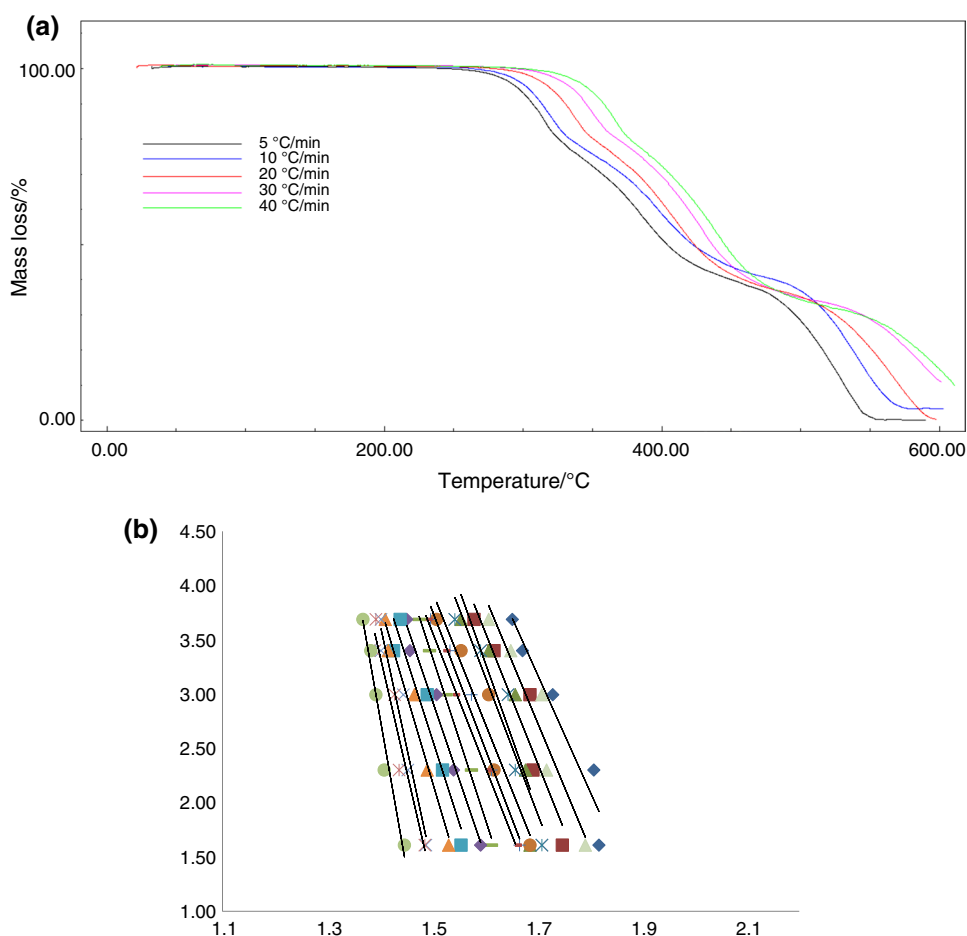


Fig. 9 Dependences E_a – α computed from the data simulated as a function of T for the decomposition of P(CUMAC-co-BA 0.54)

0.18, 0.2, 0.25, 0.3, 0.35, 0.40, 0.42, 0.45, and 0.5, respectively. The average activation energy value of P(CUMAC-co-BA 0.54) for conversion from 0.02 to 0.5 was calculated as $124.26 \text{ kJ mol}^{-1}$. The closest activation energy value for this value was seen for 35% conversion. There are some kinetics data sets based on the *International Confederation and Thermal Analysis and Calorimetry* (ICTAC) in the literature

[23]. One of these data are alpha-temperature (α – T) curves. In Fig. 9, dependences E_a are computed from the data simulated as a function of temperature (T) for the decomposition of P(CUMAC-co-BA 0.54). E_a reaches a maximum at E_a around 185 kJ mol^{-1} at $\alpha=0.42$. Generally, there is an increase in activation energy due to degradation.

As shown in Fig. 10a, b, the graphs were also drawn for the P(CUMAC-co-BA 0.32) with the same parameters. For the Flynn–Wall–Ozawa method, measurements were taken from 2 to 50% conversion values. Figure 10a shows the measured TGA curves in different heating rates of P(CUMAC-co-BA 0.32) systems. The results of Flynn–Wall–Ozawa analysis ($\ln\beta$ versus $10^3/T$) are given in Fig. 10b. From the slope of a series line obtained, the activation energy value corresponding to each conversion percentage was calculated separately. Among these values, the average activation energy value for the polymer was calculated as $93.46 \text{ kJ mol}^{-1}$. The activation energy value ($93.42 \text{ kJ mol}^{-1}$) corresponding to 8% conversion corresponds to the value closest to the average activation energy value. As shown in Fig. 11, dependences E_a – α computed from the data simulated as a function of “ T ” for the decomposition of P(CUMAC-co-BA 0.32). As the

Fig. 10 **a** TGA curves in different heating rates of P(CUMAC-co-BA 0.32) **b** extent of conversion versus temperature curves at different heating rates (5, 10, 20, 30 and 40 °C min⁻¹)

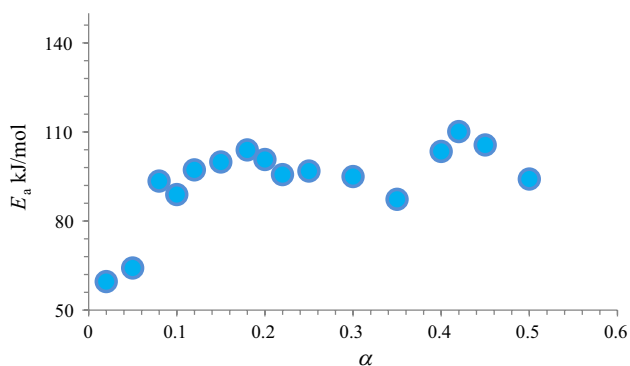
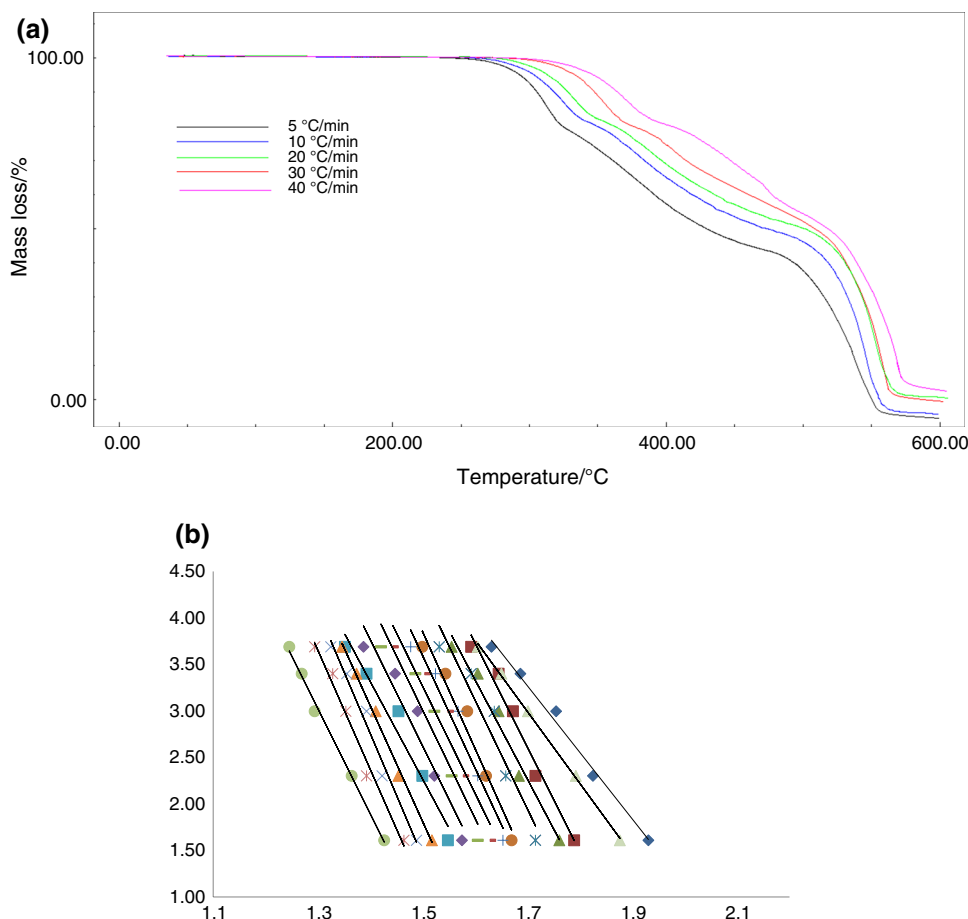


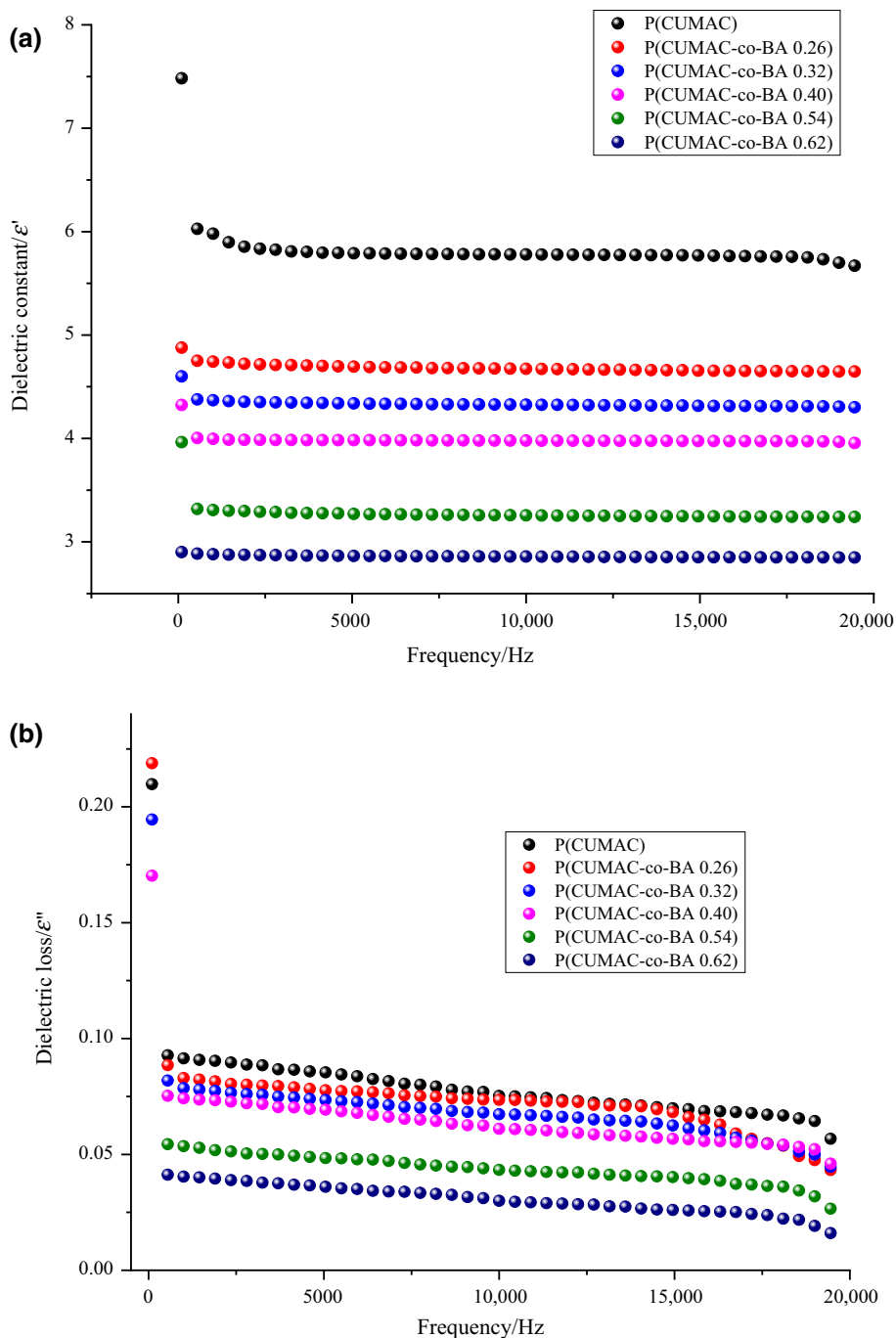
Fig. 11 Dependences $E_a - \alpha$ computed from the data simulated as a function of T for the decomposition of P(CUMAC-co-BA 0.32)

coumarin ratio in the copolymer system increases, the activation energy decreases from 124,26 kJ/mol to 93,46 kJ/mol. As a result, it is believed that the coumarin ring is easier to remove from the molecule by the effect of temperature.

Dielectric and electrical properties

Dielectric properties of a polymer can be described by dielectric constant (ϵ'), dielectric loss factor (ϵ''), and conductivity (σ_{ac}). For receive measurement, 0.1 g (co)polymer was pressed under 4 tons into disk-shaped samples with a thickness ranging from 0.96 mm to 1.5 mm. The dielectric and AC conductivity measurements were carried with a QuadTech 7600 precision LRC Meter impedance analyzer. The capacitance (C_p) and the loss factor (Df), conductance (Gp) values were measured over the frequency range 100 Hz–20 kHz. The dielectric constant was calculated from C_p (capacitance) using $\epsilon' = C_p \cdot d / \epsilon_0 \cdot A$. Here " C_p " is parallel capacitance, " ϵ_0 " is permittivity in free space ($\epsilon_0 = 8.854 \times 10^{-12}$ F/m), " d " is the thickness of the polymer sample, and A is the surface area of the sample. The dielectric loss factor is found by the formula, $\epsilon'' = \epsilon' \cdot Df$ [10, 27, 28]. Figure 12a, b indicates the frequency depending on dielectric constant (ϵ') and dielectric loss factor (ϵ'') of P(CUMAC) and CUMAC-BA copolymers system. The ϵ' value is nearly stable for all polymers over

Fig. 12 a The dielectric constant change **b** the dielectric loss factor change of polymers



1 kHz [29]. Therefore, this frequency is the most ideal value. Dielectric constants and dielectric loss factor of P(CUMAC) are 5.91, 0.090 at 1 kHz, respectively. ϵ' of copolymer system are, 4.73, 4.36, 3.99, 3.30, and 2.87, respectively. Figure 12a, b shows that ϵ' and ϵ'' values decreased with increase in frequency because of polarization effects [29–32]. So a decrease was observed in the

dielectric constant [33]. At low frequencies, orientation and interface polarizations are more influential. Therefore, the dielectric loss factor is high [29]. The same behavior is available in the dielectric loss factor. Another important point in the results is that as coumarin composition increases, the dielectric constant and dielectric loss values were higher. The reason for this is the presence of an

Fig. 13 Variation of AC log conductivity with frequency for copolymer systems

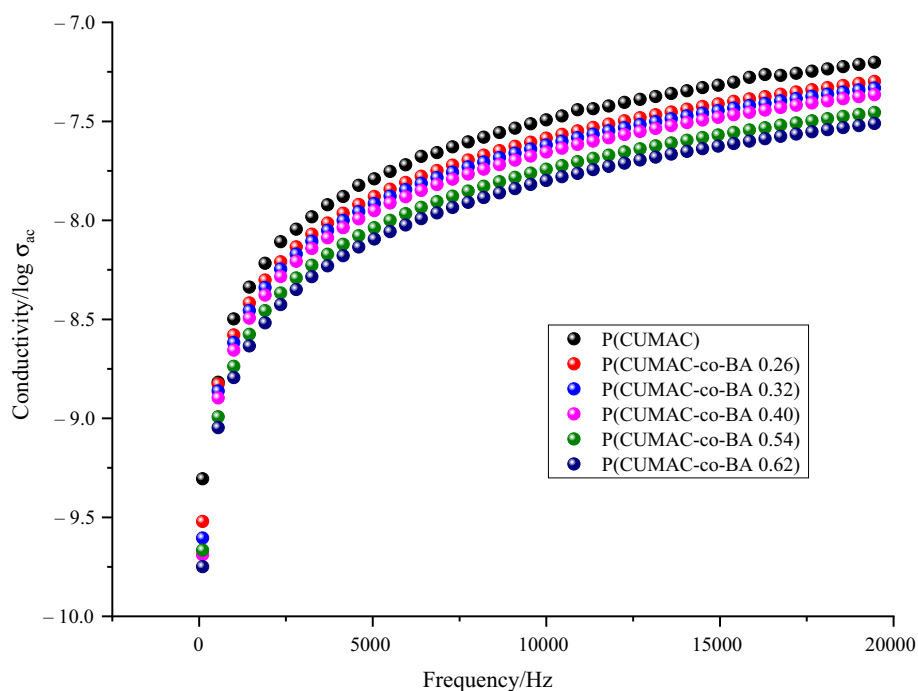


Table 2 Dielectric and electrical properties of copolymer series at 1 kHz at 25 °C

Sample	ϵ'	ϵ''	$\sigma/S \text{ cm}^{-1}$	$\log/S \text{ cm}^{-1}$
P(CUMAC)	5.91	0.090	4.16×10^{-9}	-8.38
Poly(CUMAC-co-BA 0.26)	4.73	0.082	3.42×10^{-9}	-8.46
Poly(CUMAC-co-BA 0.32)	4.36	0.078	3.14×10^{-9}	-8.50
Poly(CUMAC-co-BA 0.40)	3.99	0.073	2.87×10^{-9}	-8.54
Poly(CUMAC-co-BA 0.54)	3.30	0.052	2.38×10^{-9}	-8.62
Poly(CUMAC-co-BA 0.62)	2.87	0.040	2.08×10^{-9}	-8.68

aromatic ring in the structure of coumarin. The aromatic ring caused the structure to be polar. So, the presence of polar groups such as aromatic groups, C=O groups in CUMAC units bearing high polar group is a reason for the increase in dielectric constant. It can also be said that it increases the dielectric constant. The dielectric properties of materials related to the polar groups on the monomer units so the dielectric constant for polar materials is upper [14, 34–39].

AC (σ_{ac} , $S \text{ cm}^{-1}$) conductivity is significant for the transmission mechanism. Conductivity (σ_{ac}) values were calculated from the conductance (Gp) parameter with the help of the formula;

$\sigma_{ac} = Gp \cdot d/A$ [28] where Gp is the conductance, d is the thickness of the film, and A is the sample space. AC

conductivity (σ_{ac}) values of copolymers were researched as a function of frequency. The conductance measurements of copolymer system were studied at 100 Hz and 20 kHz depending on the alternating current (AC) conductivities. Figure 13 shows the behavior of the conductivity with frequency at room temperature. It has been observed the conductivity values increase with the frequency [40, 41]. For five different rates of CUMAC-BA copolymer systems at room temperature, the σ_{ac} value increased from 2.28×10^{-9} (at 1 kHz) to 4.16×10^{-9} (at 1 kHz) for the Poly(CUMAC-co-BA 0.26) copolymer at 25 °C. The electrical conductivity of the polymers depends on freeloards (electrons or ions) in their structures and their mobility in the structure [42, 43]. The ϵ' , ϵ'' , and σ_{ac} data for copolymer system are summarized in Table 2.

Thermal decomposition on dielectric properties of copolymer system

It is thought that there will be changes in the dielectric value of the residual polymer structures at different temperatures. For this purpose, dielectric behaviors of residues were determined after heating to the first decay temperature of the two-stage decay polymers and compared with the first states. Thus, the effect of thermal degradation was investigated on dielectric behaviors of copolymers. The dielectric constants (ϵ'), the dielectric loss factor (ϵ''), and ac conductivity (σ_{ac}) of residual

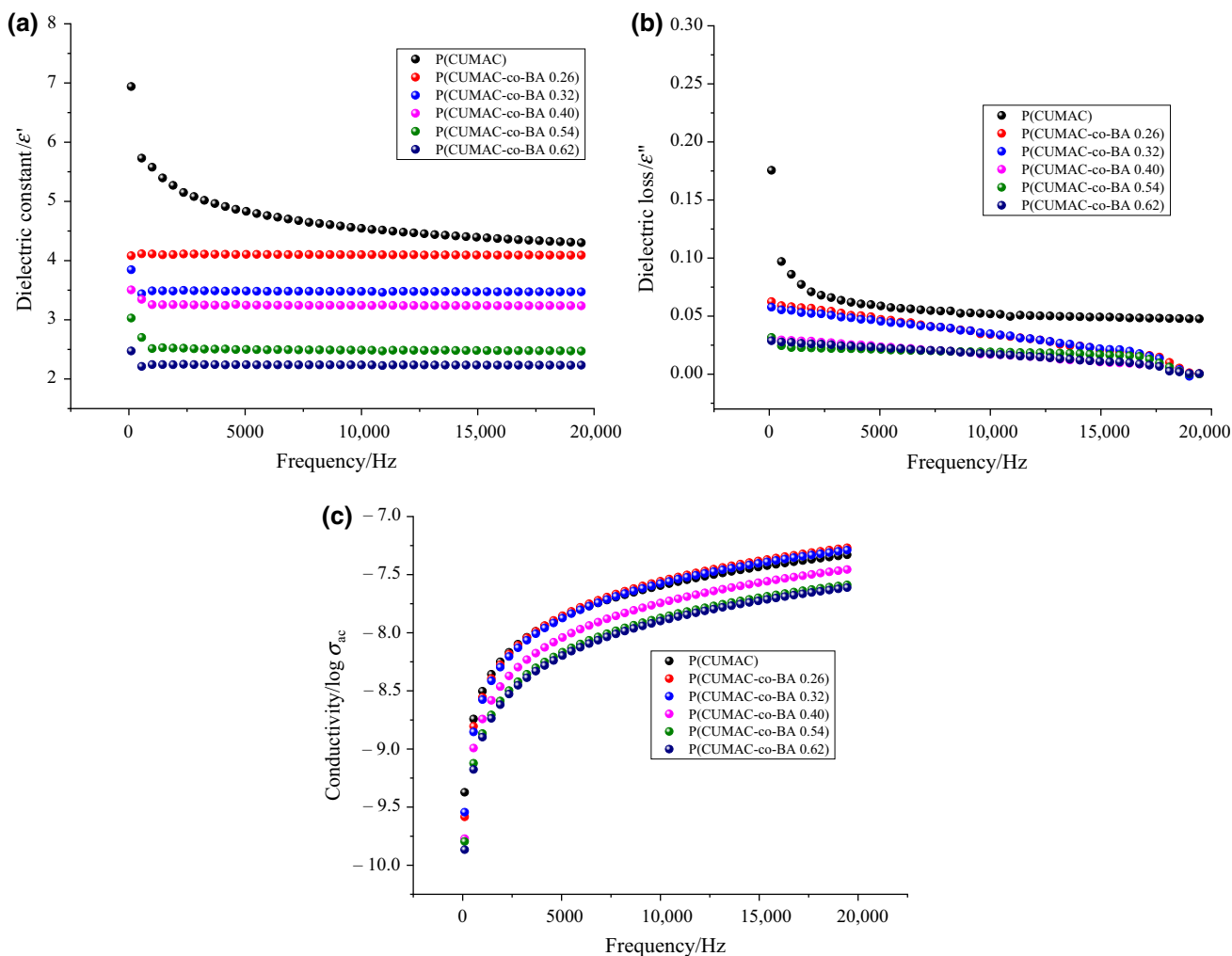


Fig. 14 **a** Dielectric constant graph, **b** dielectric loss factor, **c** σ_{ac} of residual polymer frequency dependence at 1 kHz of at 320 °C

Table 3 Dielectric and electrical properties of residual polymer at 320 °C of copolymer series at 25 °C

Sample	ϵ'	ϵ''	$\sigma/S\text{ cm}^{-1}$	$\log/S\text{ cm}^{-1}$
P(CUMAC)	5.50	0.081	3.56×10^{-9}	-8.44
Poly(CUMAC-co-BA 0.26)	4.11	0.057	3.20×10^{-9}	-8.49
Poly(CUMAC-co-BA 0.32)	3.49	0.054	3.05×10^{-9}	-8.51
Poly(CUMAC-co-BA 0.40)	3.25	0.028	2.08×10^{-9}	-8.68
Poly(CUMAC-co-BA 0.54)	2.51	0.022	1.56×10^{-9}	-8.80
Poly(CUMAC-co-BA 0.62)	2.24	0.027	1.45×10^{-9}	-8.83

polymer structures depending on frequency have been studied at 1 kHz for residual P(CUMAC) and CUMAC-BA copolymer systems partially degraded to 320 °C, and related curves are displayed in Fig. 14a–c and are summarized in Table 3.

Dielectric properties of P(CUMAC) and its residue at 320 °C was showed in Fig. 15a–c. At 1 kHz, ϵ' and ϵ'' values decrease with increase in frequency for both P (CUMAC) and its residual polymer at 320 °C. Dielectric and electrical values (ϵ' , ϵ'' , σ_{ac}) of residual homopolymer had a lower value. This is thought to be the result of the breakdown of the coumarin ring in the structure of the polymer at 320 °C. Therefore, the polarity of the structure decreased and dielectric and electrical values decreased. In the frequency range, dielectric constants, dielectric loss factor, and conductivity were calculated as 5.50, 0.081, and $3.56 \times 10^{-9}\text{ S cm}^{-1}$ for P (CUMAC), which is partially degraded at 320 °C, respectively.

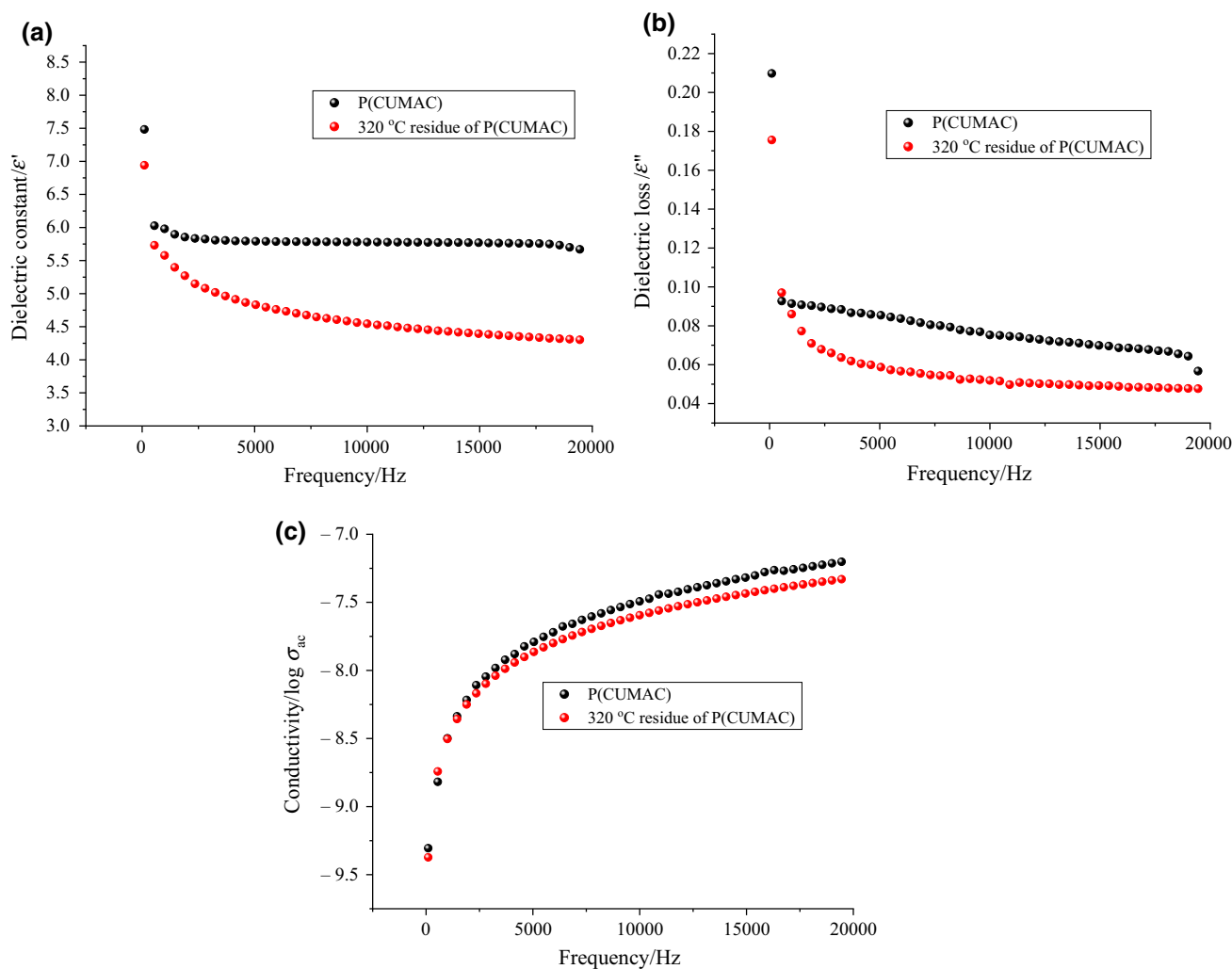


Fig. 15 **a** Dielectric constant, **b** dielectric loss factor, **c** σ_{ac} of P(CUMAC) and its residual polymer at 320 °C frequency dependence at 1 kHz of at 25 °C

Conclusions

New coumarin copolymers of poly(CUMAC-*co*-BA) were synthesized and characterized. The thermal behavior of copolymers was investigated by thermogravimetric analysis (TGA). The kinetics of thermal decomposition with two stages of poly(CUMAC-*co*-BA) was estimated from a series of experiments at five heating rates. The activation energies of the copolymers were calculated as 124.26 kJ mol⁻¹–93.46 kJ mol⁻¹ according to FWO method. The dielectric measurements were measured by means of an impedance analyzer as a function of temperature and frequency. According to these results, the side group elimination in the polymer chain is higher in the coumarin containing mer. This reduces the activation energy and it accelerates the degradation. In addition, a clear decrease is observed in the dielectric properties of the remains at 320 °C. The

reason for this decrease is thought to be the separation or breakdown of the polar and voluminous Cl-coumarin group in the structure.

References

- Peterson JD, Vyazovkin S, Charles A. Wight, kinetics of the thermal and thermo-oxidative degradation of polystyrene, polyethylene and poly(propylene). *Macromol Chem Phys.* 2001;202:775–84.
- Madorsky SL. Thermal degradation of organic polymers. New York: Interscience Publishers; 1964.
- Zaikov GE. Degradation and stabilization of polymers: theory and practice. Nova Science Publishers, Commack, New York; 1995.
- Kurt A. Thermal decomposition kinetics of poly(nButMA-*b*-St) diblock copolymer synthesized by ATRP. *J Appl Polym Sci.* 2009;114:624–9.

- Venkatesh M, Ravi P, Surya P. Tewari isoconversional kinetic analysis of decomposition of nitroimidazoles: Friedman method vs. Flynn–Wall–Ozawa method. *J Phys Chem A*. 2013;117:10162–9.
- Longfei G, Haibin Z, Yajie W, Jun Z. Thermal behavior and kinetic study on the pyrolysis of lean coal blends with thermally dissolved coal. *J Therm Anal Calorim*. 2019;136:903–12.
- Blainea RL, Kissinger HE. Homer Kissinger and the Kissinger equation. *Thermochim Acta*. 2012;540:1–6.
- Budrugaec P, Segal E. Applicability of the Kissinger Equation in thermal analysis. *J Therm Anal Calorim*. 2007;88:703–7.
- Biryán F, Demirelli K. A methacrylate monomer bearing nitro, aryl, and hydroxyl side groups: homopolymerization, characterization, dielectric, and thermal degradation behaviors. *J Appl Polym Sci*. 2016;133:43925.
- Yakuphanoglu F, Okutan M, Zhuang Q, Han Z. The dielectric spectroscopy and surface morphology studies in a new conjugated polymer poly(benzobisoxazole-2,6-diylvinylene). *Physica B*. 2005;365:13–9.
- Santana L, Teijeira M, Uriarte E, Teran C, Liñares B, Villar R, Laguna R, Cano E. AM1 theoretical study, synthesis and biological evaluation of some benzofuran analogues of anti-inflammatory arylalkanoic acids. *Eur J Pharm Sci*. 1999;7:161–6.
- Biryán F, Demirelli K. Copolymerization of Benzyl methacrylate and a methacrylate bearing, benzophenoxy and hydroxyl side groups: monomer reactivity ratios, thermal studies and dielectric measurements. *Fibers Polymers*. 2017;18:1629–37.
- Mao Z, Zhang J, Toughening J. Effect of CPE on ASA/SAN binary blends at different temperatures. *Appl Polym Sci*. 2016;133:43353–60.
- Biryán F, Demirelli K. Thermal degradation kinetic, electrical and dielectric behavior of brush copolymer with a polystyrene backbone and polyacrylate-amide side chains/nanographene-filled composites. *J Mol Struct*. 2019;1186:187–203.
- Liu P, Zhen W. Structure-property relationship, rheological behavior, and thermal degradability of poly(lactic acid)/fulvic acid amide composites. *Polym Adv Technol*. 2018;29:2192–203.
- Vyazovkin S. Modification of the integral isoconversional method to account for variation in the activation energy. *J Comput Chem*. 2001;22:178–83.
- Peterson JD, Vyazovkin S, Wight CA. Kinetics of the thermal and thermooxidative degradation of polystyrene polyethylene and poly(propylene). *Macromol Chem Phys*. 2001;202:775–84.
- Acquah C, Danquah MK, Moy CKS, Anwar M, Ongkudon CM. Thermogravimetric characterization of ex situ, polymethacrylate (EDMA-co-GMA) monoliths. *Can J Chem Eng*. 2017;9999:1–7.
- Kurt A, Ayaz H, Gültek A. Investigation of thermal degradation kinetics of pyrazabole centered two-armed poly(methyl methacrylate). *Adıyaman Univ J Sci*. 2016;6:233–51.
- Nunez L, Fraga F, Nunez MR, Villanueva M. Thermogravimetric study of the decomposition process of the system BADGE ($n=0$)/1,2 DCH. *Polymer*. 2000;41:4635–41.
- Flynn JH, Wall LA. General treatment of the thermogravimetry of polymers. *J Res Nat Bur Stand A Phys Chem*. 1966;70:487–523.
- Ozawa T. A new method of analyzing thermogravimetric data. *Bull Chem Soc Jpn*. 1965;38:1881–6.
- Biryán F, Demirelli K. Characterization, thermal behavior, and electrical measurements of poly[4-(2-bromoisobutyryl methyl)styrene]. *Adv Polym Technol*. 2018;37:1994–2012.
- Newkirk AE. Thermogravimetric measurements. *Anal Chem*. 1960;32:1558.
- Waters DN, Paddy JL. Equations for isothermal differential scanning calorimetric curves. *Anal Chem*. 1988;60:53–7.
- Vyazovkin S, Chrissafis KD, Lorenzo ML, Koga N, Pijolat M, Roduit B, Sbirrazzuoli N, Sunol J.J. ICTAC Kinetics Committee recommendations for collecting experimental thermal analysis data for kinetic computations. *Thermochim Acta*. 2014; 590:1
- Seven P, Coskun M, Demirelli K. Synthesis and characterization of two-armed graft copolymers prepared with acrylate and methacrylate using atom transfer radical polymerization. *React Funct Polym*. 2008;68:922–30.
- Rajendran S, Ramesh PM. Effect of different plasticizer on structural and electrical properties of PEMA-based polymer electrolytes. *J Appl Electrochem*. 2010;40:327–32.
- Biryán F, Demirelli K. Temperature-frequency dependence on electrical properties of EuCl₃ based composites, thermal behaviors and preparation of poly(3-acetamidopropyl acrylate). *Ferroelectrics*. 2018;526:76–94.
- Patel PK, Rani J, Adhlakha N, Singh H, Yadav KL. Enhanced dielectric properties of doped barium titanate ceramics. *J Phys Chem Solids*. 2013;74:545.
- Simpson JO, Clair AKS. Fundamental insight on developing low dielectric constant polyimides. *Thin Solid Films*. 1997;308–309:480–5.
- Ayaz N, Bezgin F, Demirelli K. Polymers based on methacrylate bearing coumarin side group: synthesis via free radical polymerization, monomer reactivity ratios, dielectric behavior, and thermal stabilities. *ISRN Polym Sci*. 2011;2012:1–13.
- Belakere NN, Misra SCK, Ram MK, Rout DK, Gupta R, Malhotra BD, Chandra S. Interfacial polarization in semiconducting polypyrrole thin-films. *J Phys: Condens Matter*. 1992;4:5747–56.
- Ramesh S, Yahana AH, Aroof AK. Dielectric behaviour of PVC-based polymer electrolytes. *Solid State Ionics*. 2002;291:152–3.
- Biryán F, Abubakar AM, Demirelli K. Product analysis, electrical and dielectric properties depending on thermal influence of poly(N-isopropyl acrylamide)/graphite-filled composite. *Thermochim Acta*. 2018;669:66–79.
- Saafan SA, Ayad MM, El-Ghazzawy EH. The effect of preparation conditions on the growth rate of films, the yield of precipitated powder and the DC conductivity of polypyrrole. *Turk J Phys*. 2005;29:355–62.
- Açıkses A, Çömez N, Biryán F. Preparation and characterization of styrene bearing diethanolamine side group, styrene copolymer systems, and their metal complexes. *Int J Polym Sci*. 2018; Article ID 6703783: 15 p. <https://doi.org/10.1155/2018/6703783>.
- Stefanec D, Krajnc P. 4-Vinylbenzyl chloride based porous spherical polymer supports derived from water-in-oil-in-water emulsions. *React Funct Polym*. 2005;65:37–45.
- Tareev B. *Physics of dielectric materials*. Moscow: MIR Publications; 1979.
- Biryán F, Demirelli K, Torğut G, Phtılı G. Synthesis, thermal degradation and dielectric properties of poly[2-hydroxy,3-(1-naphthoxy)propyl methacrylate]. *Polym Bull*. 2017;74:583–602.
- Ku CC, Liepins R. *Electrical properties of polymers: chemical principles*. Munich: Hanser; 1987. p. 11.
- Alkan Ü. Investigation of mechanical and electrical properties of polymer composites under the influence of stabilizing and corrosive factors., Ph.D. Thesis, Yildiz Technical University, Graduate School of Natural and Applied Sciences, 2011; p. 130.
- Tager A. *Physical chemistry of polymers*. English Translation, MIR Publishers. 1978.

Publisher's Note Springer Nature remains neutral with regard to jurisdictional claims in published maps and institutional affiliations.